Regular Article

INORGANIC CHEMISTRY RESEARCH
Published by the
Iranian Chemical Society
www.inorgchemres.org
info@inorgchemres.org

Inorg. Chem. Res., Vol. 5, No. 1, 120-131, June 2021
DOI: 10.22036/icr.2021.266085.1100

A DFT Study of Selenium-Cyclic Peptide Anticancer Nanocarrier

Sara Moghimi[a], Ali Morsali[a,b,]*, Mohammad M. Heravi[a] and S. Ali Beyramabadi[a,b]

[a]*Department of Chemistry, Mashhad Branch, Islamic Azad University, Mashhad, Iran*
[b]*Research Center for Animal Development Applied Biology, Mashhad Branch, Islamic Azad University, Mashhad 917568, Iran*
(Received 6 January 2021, Accepted 1 February 2021)

Using Se8 selenium and cyclic peptides nanoparticles (SeCPNP), six configurations for the adsorption of the 5-fluorouracil (FU) anticancer drug on SeCPNP have been examined (SeCPNP/FU1-6). Binding energies, solvation energies and quantum molecular descriptors such as electrophilicity (ω) and global hardness (η) in the aqueous solution and gas phase were studied at the density functional level of M06-2X. The most stable structure by binding energy calculations was determined. The values obtained from solvation energies indicate that SeCPNPs can increase the solubility of FU, which is a key factor in drug delivery. According to quantum molecular descriptors, the reactivity of cyclic peptide (CP) and FU drug in all structures (SeCPNP/FU 1-6) increases. AIM calculations for all structures show that Se-A interactions (A = O, H, N, F and C) and intermolecular hydrogen bonding play an important role for this drug delivery system. In structures where FU is parallel to SeCPNP and undergoes interactions concurrently with Se8 and CP, it is more stable than structures in which the drug undergoes interactions only with Se8 and CP.

Keywords: 5-Fluorouracil, Anticancer, AIM analysis, DFT, Selenium cyclic peptide nanoparticles

INTRODUCTION

Cyclic peptides have many usages in various contexts such as drug delivery, nanoscience, optical sensors, and electronic devices. The cyclic structure of these compounds with different chain amino acids is a good pattern for encapsulating medicines [1-4]. Cyclic peptides are polypeptide chains that would be as a cyclic structure. The cyclic structure of these compounds with different chain amino acids is a very good pattern for surrounding medicines [5]. The ring structure is formed by the end of one peptide to the other section with an amide bonding. Peptides are less toxic than synthetic molecules and therefore do not accumulate in the tissue. Cyclic peptide-based drugs can cause less harm. Cyclic peptides usually show better biological activities than their linear counterparts due to their rigid configuration. Cyclic peptides have a variety of structural properties leading to their use as a target drug binder in medical applications [6,7]. The compatibility of cyclic peptides provides the ability and stability of cell permeability compared to its linear counterparts. Over the past few years, the use of cyclic peptides in the transport of a wide range of therapeutic agents (including anticancer drugs, anti-HIV drugs, and essential phosphopeptides) has been investigated [8-11].

Cancer is a serious threat to human health and economic and social development and it has become one of the most important public health problems in the world. Once the tumor is found in the advanced stage, and it spreads very widely reaching a stage requiring treatment methods including surgery, radiotherapy, and chemotherapy. Commonly used chemotherapy drugs include 5-fluorouracil [12,13], gemcitabine [14,15] and doxorubicin [16]. 5-Fluorouracil is widely used in the treatment of cancer. Although this drug was introduced more than thirty years ago, it is still one of the most widely used anti-cancer drugs for the treatment of many different malignant cancers alone or with other drugs; it shows a soothing activity in breast,

*Corresponding author. E-mail: almorsali@yahoo.com

gastrointestinal (especially colon cancer) and ovarian cancers [12,17-19]. Nevertheless, its half-life is only 10 to 15 min and retention time in the body is short [20].

Impressive delivery of medicines to target locations significantly improves their remedial power. Drug delivery systems (DDS) as a modern tool for boosting the features of drugs have recently been recommended. For boosting drug stability and availability, cell uptake, and reduce toxicity, many DDSs are made from a variety of materials such as inorganic nanoparticles [21-24], nanotubes [25,26], polymers [27,28], peptides [29] and liposomes [30]. Nano-DDS-based drug delivery systems have multiple benefits compared with larger DDSs, such as lower toxicity and recovered cell uptake [31]. Peptides are generally applied as nanoscale systems to deliver drugs because of their capability to transport an extensive range of molecules by encapsulating the medicine (surrounding). Furthermore, peptides are applied as section of the structure of nano-DDS by a widespread range of amino acids with various physicochemical characteristics. For example, peptides functionalized with gold nanoparticles have been applied as one of the earliest biochemical systems in drug delivery and to improve cell transfer of several drugs by non-covalent complexation [32].

Among the diverse metal nanoparticles, selenium nanoparticles (SeNPs) have not been extensively investigated. As an essential metal, 55 mg of selenium is ingested daily from the diet [33]. Selenium is also needed for cellular operation. Extra doses of selenium can lead to cell death [34]. Therefore, in fact, it is essential to design new SeNPs that can be applied as non-toxic nano-DDSs. SeNPs are coated or functionalized with alternative compounds to recover their biological attributes. The size of nanoparticles is a key factor that can change their biological activity. The amount of consumption and chemical form of selenium is very significant to reduce toxicity and increase remedial effects [35].

Quantum chemical studies help design and analyze drug delivery systems [36-39]. The 2016 Nobel prize was awarded for the designing, manufacturing and delivery of drug [40,41]. Rather than experimental methods, theoretical procedures are principal gadgets for studying medicine delivery systems. In this research, density function theory (DFT) was applied to evaluate the performance of cyclic peptide selenium nanoparticles (SeCPNPs) by the anticancer medicine of 5-fluorouracil (FU).

COMPUTATIONAL METHOD

All calculations were done by 6-31G(d,p) basis set and at the density functional level of M06-2X [42,43] and using GAUSSIAN 09 software [44]. The structure of all configurations was optimized. In this study, the effects of solvent were investigated using the polarized continuum model (PCM) [45,46]. Solvent energy was calculated using the following equation:

$$\Delta E_{solv} = E_{sol} - E_{gas} \quad (1)$$

E_{sol} and E_{gas} indicate the total energy of the solution and gas phases. Calculations were done for 5-fluorouracil, cyclic peptide (CP), selenium nanoparticles (SeNPs) and its six configurations.

Quantum molecular descriptors were applied to evaluate chemical reactivity and stability. Hardness (η) indicates insistence to changing electronic structure (Eq. (2)).

$$\eta = \frac{I - A}{2} \quad (2)$$

In fact, $I = -E_{HOMO}$ is the ionization energy and $A = -E_{LUMO}$ is the amount of electron affinity of the molecule. The lowest unoccupied molecular orbital is LUMO and the highest occupied molecular orbital is HOMO. The difference in energy of E_{HOMO} and E_{LUMO} is the gap of energy (E_{gap}). The higher the E_{gap}, the more stable the structure. The electrophilicity index (ω) is determined by Parr as Eq. (3) [47].

$$\omega = \frac{(I + A)^2}{8\eta} \quad (3)$$

We investigated hydrogen bonding using QTAIMs (Quantum Theory of Atoms in Molecule) calculations. AIM calculations are performed using AIMAII software [48]. QTAIM is based on analyzing the electron density ρ(r) topology [49]. We perused different contents of electron density such as kinetic energy (G_b), energy density (V_b), total

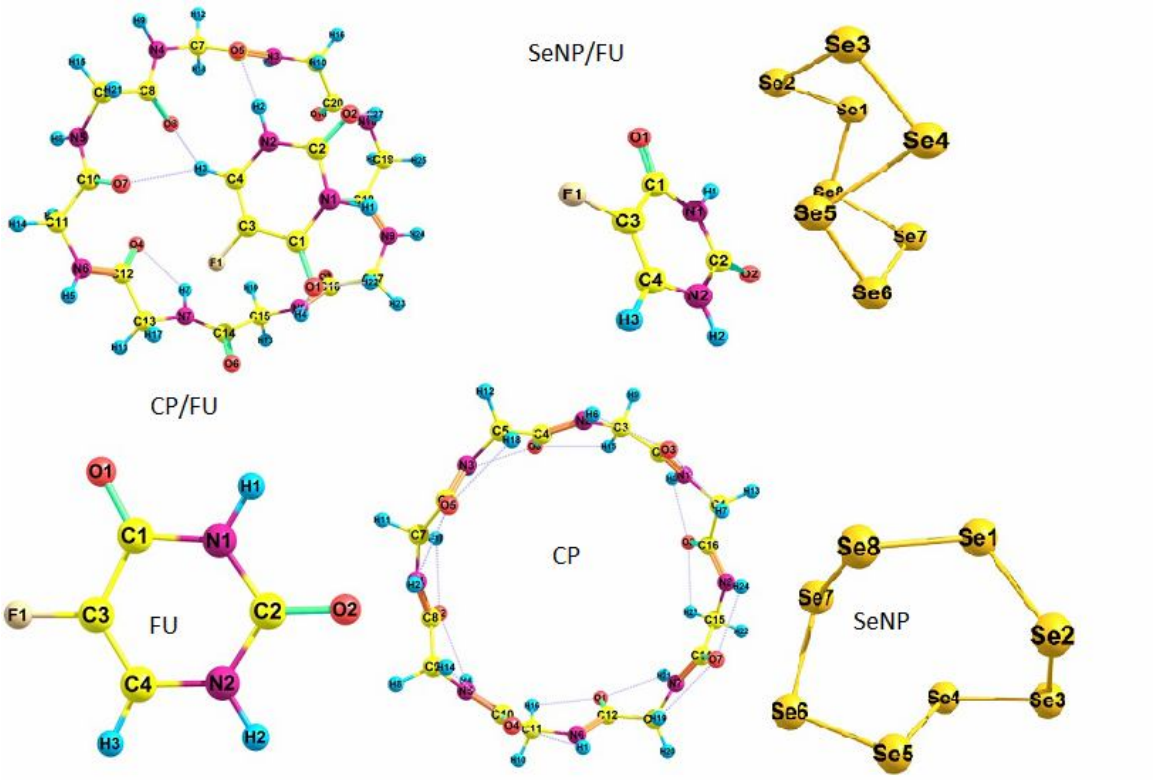

Fig. 1. Optimized structures of FU, SeNP, CP, SeNP/FU and CP/FU.

energy density (H_b) and electron density of Laplacian ($\nabla^2\rho$) at a bond critical point (BCP) for differentiating the nature of bonding in various species.

RESULTS AND DISCUSSION

Binding and Solvation Energies

In this study, selenium nanoparticles (SeNPs) and cyclic peptide (CP) respectively, from the cyclic Se8 model [50,51] and the cyclooctaglycine model [52] with the 5-fluorouracil drug (FU), which have CH, CF, CO and NH groups, were used, as shown in Fig. 1. The interaction of 5-fluorouracil with selenium-peptide nanoparticles has been considered from 6 different directions (SeCPNP/FU1-6). The optimized geometry of SeCPNP/FU1-6 in aqueous solution at M06-2X/6-31G** is indicated in Figs. 2 and 3. The cartesian coordinates and absolute energies of all optimized structures were presented in the Electronic Supplementary Information. Binding energies (ΔE) are computed by the following equation:

$$\Delta E = E_{SeCPNP/flo1-6} - (E_{CP} + E_{SeNP} + E_{FU}) \quad (4)$$

Table 1 shows the binding energies in the gas phase and aqueous solution at M06-2X. Dispersion interactions are spotted by this level [53]. The energies (ΔE) liaise on the orientation of the medicine relative to SeCPNP. In the gas phase, among 6 species, SeCPNP/FU6 is the most stable structure and in the solution phase, SeCPNP/FU2 is the most stable structure in which the 5-fluorouracil is parallel to SeCPNP and the NH functional group interacts with the SeCPNP functional groups (Fig. 2). According to the most stable configuration, the structure of 5-fluorouracil is optimized separately near CP (CP/FU) and SeNP (SeNP/FU). The optimized structures of these configurations have been showed in Fig. 1. Comparison of binding energies (Table 1) shows that encapsulation of SeNP within CP

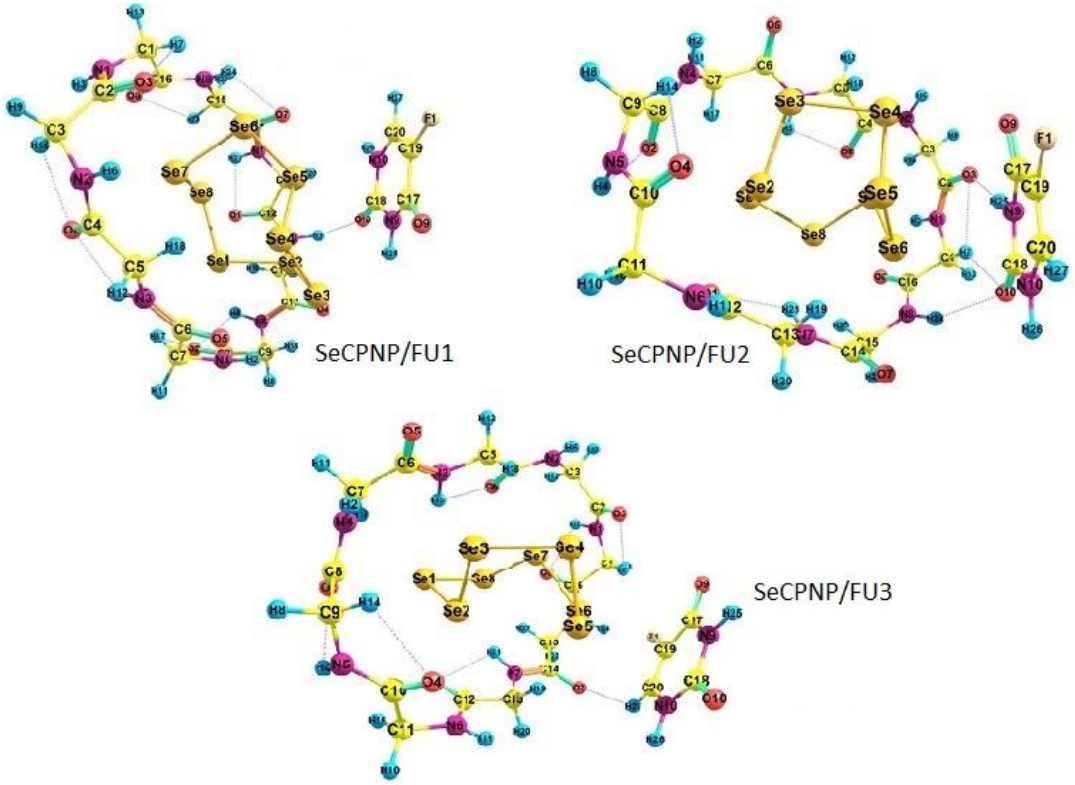

Fig. 2. Optimized structures of SeCPNP/FU1-3.

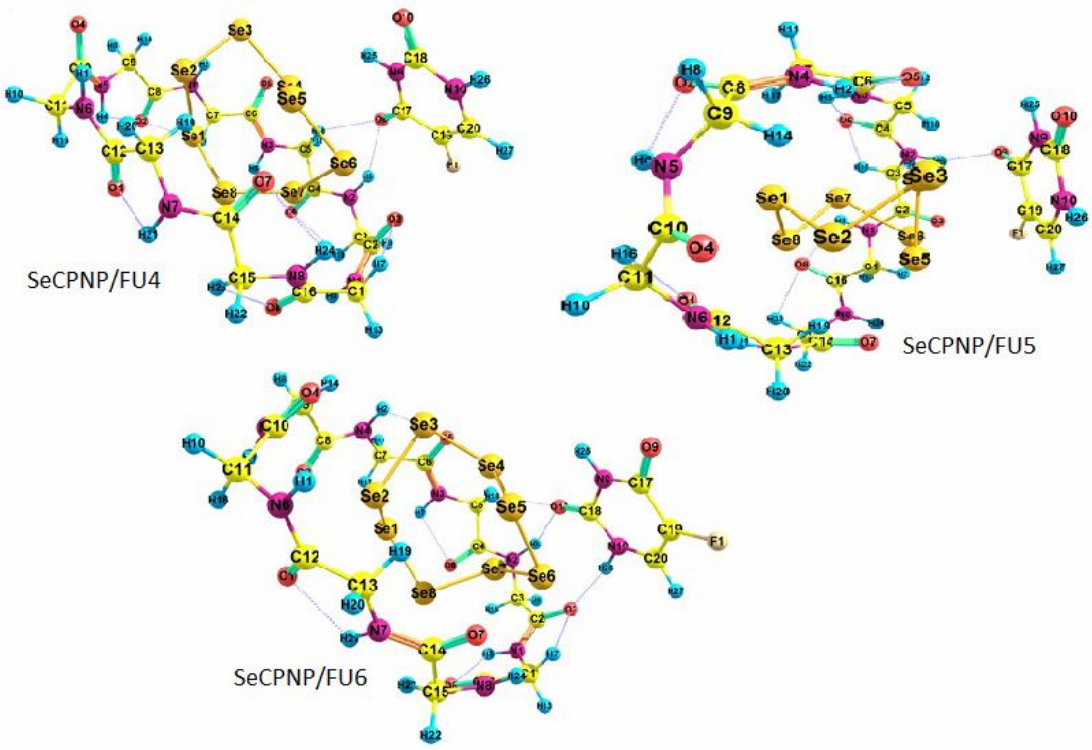

Fig. 3. Optimized structures of SeCPNP/FU4-6.

Table 1. Binding and Solvation Energy Values (kJ mol^{-1}) for Corresponding Structures

Species	ΔE_{gas}	ΔE_{H2O}	ΔE_{solv}
FU	-	-	-40.95
CP	-	-	-92.22
SeNP	-	-	-9.66
CP/FU	-208.85	-119.75	-44.08
SeNP/FU	-110.01	-101.54	-36.99
SeCPNP/FU1	-478.30	-480.17	-144.71
SeCPNP/FU2	-554.86	-499.69	-87.67
SeCPNP/FU3	-531.75	-472.54	-83.63
SeCPNP/FU4	-554.86	-481.32	-69.30
SeCPNP/FU5	-573.43	-498.69	-68.09
SeCPNP/FU6	-573.65	-492.78	-61.97

boosts binding energy, though this operation is sometimes weaker in aqueous solutions than in the gaseous phase.

We appraised the solvation energy for all species (Table 1). These values are negative showing that the dissolution process is spontaneous. Uptake of FU in SeCPNP increases the solvation of the drug, which is a necessary factor for its use as an effective anticancer medicine. The solvation of the medicine in the presence of SeCPNP enhances from -40.95 kJ mol^{-1} to -87.67 kJ mol^{-1} (mean value for SeCPNP/FU1-6). After activation of SeCPNP with FU, the solvation of SeNP increases, which is extremely significant in drug delivery systems. The presence of CP is the main proof for the increased solvation of SeNP and FU. Hence, in addition to reducing the toxicity of SeNP (next section), CP enhances its solvation, which is a main issue in targeted drug delivery. SeNP and CP complement each other, SeNP boosts the binding energies, and CP boosts the solubility.

Quantum Molecular Descriptors

According to the information in Table 2, in both the gas and solution phases, the values of E_g and η are almost similar between the SeCPNP/FU1-6 structures. E_g and η values increase in the presence of drug and cyclic peptide in both phases, indicating less reactivity and greater stability of these structures. Drug-related E_g and η are higher than those of SeCPNP/FU1-6 configurations, indicating that medicine reactivity increases in the presence of selenium nanoparticles and cyclic peptide.

Since electrophilicity is applied to portend toxicity, it can be said that the degree of toxicity decreases in the presence of cyclic peptide. It can also be said that the amount of ω for the solution phase is less than the gas phase. ω increases in the presence of selenium nanoparticles, indicating that in the presence of SeNP, the drug reactivity increases. ω values of FU are less than SeCPNP/FU1-6, revealing that the FU is an electron acceptor.

QTAIM Analysis

Using AIM analysis, a general study on the nature and strength of bonding interactions is done by analyzing the critical points of bond using AIM analysis. One of the

Table 2. Quantum Molecular Descriptors (eV) for Optimized Geometries

Species	E_{HOMO}	E_{LUMO}	E_g	η	ω
			H_2O		
Se	-1.64	-7.18	5.54	2.77	3.51
FU	-8.07	-0.11	7.95	3.97	2.10
CP	1.39	-8.49	9.89	4.94	1.27
CP/FU	-8.25	-0.35	7.89	3.94	2.34
SeNP/FU	-7.10	-1.54	5.55	2.77	3.36
SeCPNP/FU1	-6.91	-1.39	5.51	2.75	3.13
SeCPNP/FU2	-7.00	-1.63	5.37	2.68	3.46
SeCPNP/FU3	-7.11	-1.69	5.42	2.71	3.57
SeCPNP/FU4	-6.85	-1.39	5.45	2.72	3.12
SeCPNP/FU5	-6.82	-1.45	5.37	2.68	3.18
SeCPNP/FU6	-6.88	-1.26	5.61	2.80	2.95
			Gas		
Se	-1.74	-7.23	5.49	2.74	3.66
FU	-8.24	-0.11	8.13	4.06	2.14
CP	1.34	-8.57	9.91	4.9	1.31
CP/FU	-8.08	-0.19	7.89	3.94	2.16
SeNP/FU	-7.15	-1.71	5.44	2.72	3.61
SeCPNP/FU1	-6.91	-1.63	5.28	2.64	3.45
SeCPNP/FU2	-7.10	-1.72	5.37	2.68	3.61
SeCPNP/FU3	-6.64	-1.24	5.39	2.69	2.88
SeCPNP/FU4	-7.10	-1.72	5.37	2.68	3.62
SeCPNP/FU5	-6.97	-1.42	5.54	2.77	3.17
SeCPNP/FU6	-6.76	-1.26	5.49	2.74	2.93

parameters of electron density is (ρ(r)), which shows the potency of a bond. If the amount of (ρ(r)) is high, it means that the related bond is stronger. Laplacian of electron density ($\nabla^2\rho$) indicates the nature of a bond. A positive value ($\nabla^2\rho$) demonstrates a decline in electron density for the interaction of closed layer systems such as ion interaction, hydrogen bonding and van der Waals interactions; in contrast, negative values ($\nabla^2\rho$) demonstrate that the electron

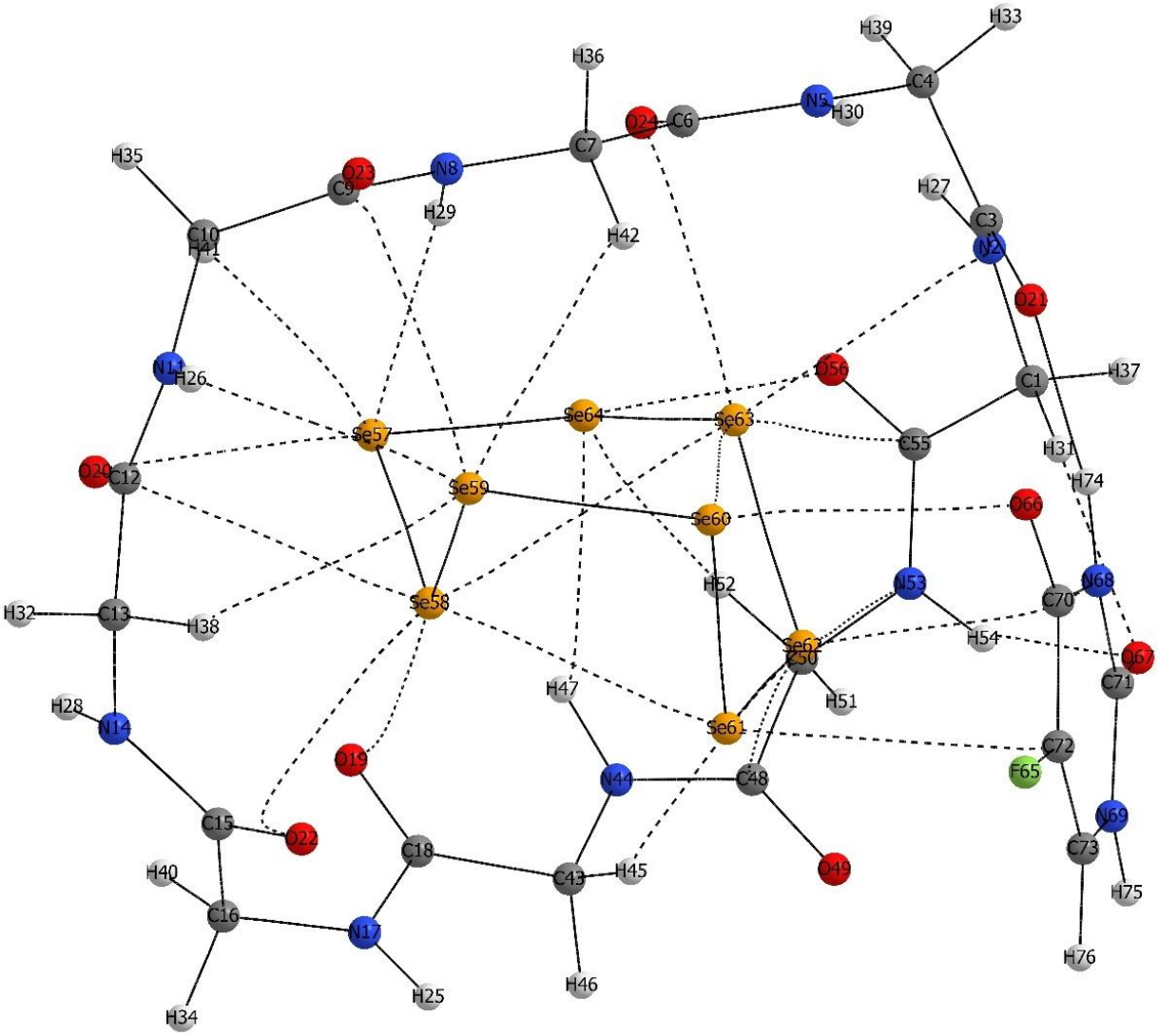

Fig. 4. Molecular diagram of SeCPNP/FU2. Lines and small green spheres correspond to the bond paths and BCP.

density in the inter-nuclear zone is concentrated, which is characterized by shared interactions or covalent bonds. If ($\nabla^2\rho < H_b < 0$) $\nabla^2\rho < 0$, $H_b < 0$) and ($\nabla^2\rho > 0$, $H_b < 0$) and ($\nabla^2\rho > 0$, $H_b > 0$), the interactions will be strong, medium and weak, respectively, and for the parameter $-G_b/V_b$ if $-G_b/V_b > 1$, $0.5 < -G_b/V_b < 1$, $-G_b/V_b < 0.5$, the bonds will be non-covalent, partially covalent and covalent, respectively [54].

The structure of SeCPNP/FU2 is reported as the most stable configuration in aqueous solution and the structure of SeCPNP/FU3 as the most unstable configuration. The molecular diagrams for SeCPNP/FU2 and SeCPNP/FU3 in aqueous solution are displayed on Figs. 4 and 5, respectively. The values of-G_b/V_b, V_b, G_b, H_b, $\nabla^2\rho(r)$, $\rho(r)$ related to SeCPNP/FU2 and SeCPNP/FU3 at the bond critical points are given in Tables 3 and 4, respectively. Hydrogen bonding energies can be calculated with $E_{HB} = 0.5V_b$ [55]. According to Table 3, in selenium nano particles, Se-Se bonds with $\nabla^2\rho < 0$, $H_b < 0$, $-G_b/V_b < 0.5$ are categorized as strong

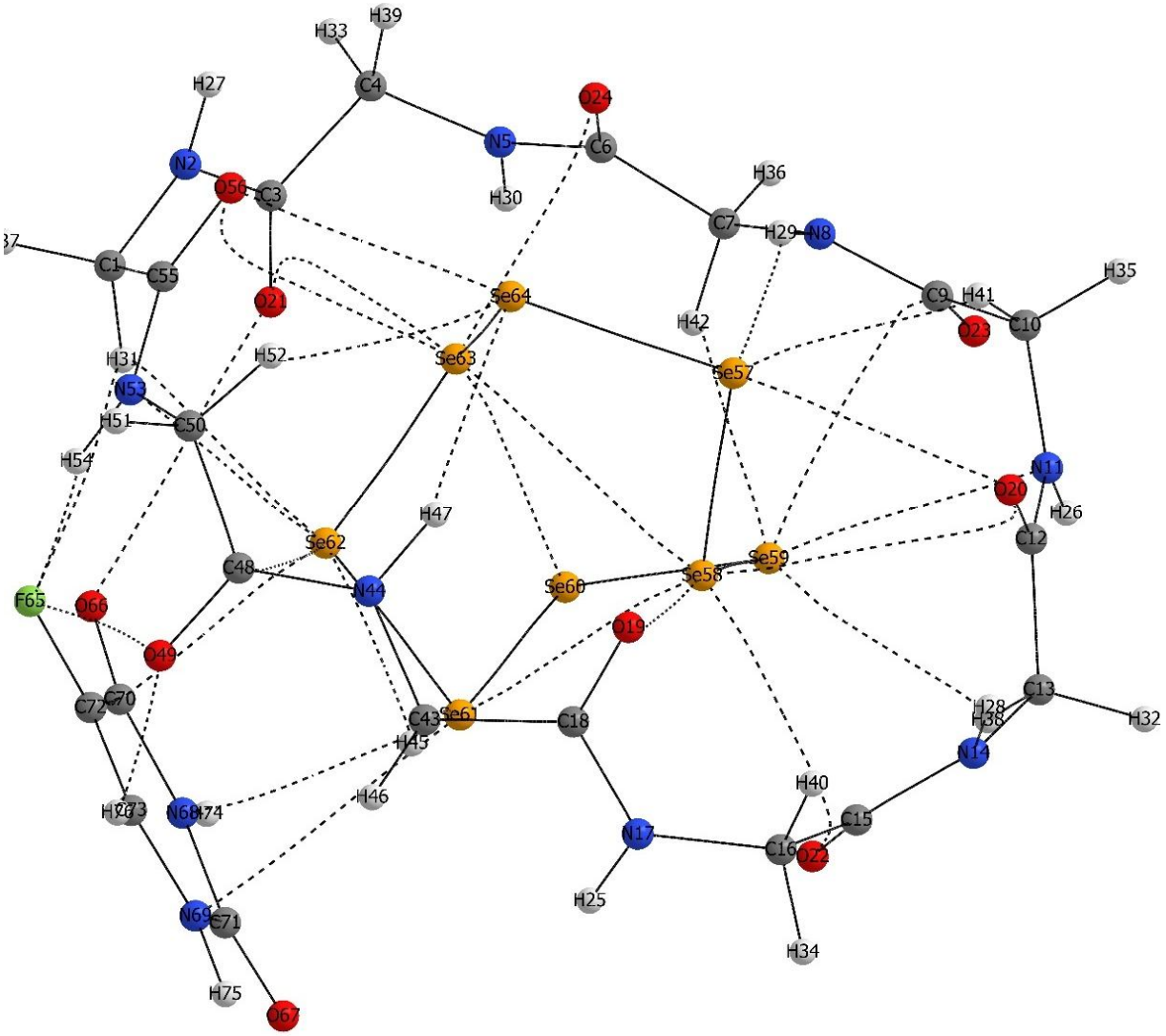

Fig. 5. Same as Fig. 4 for SeCPNP/FU3.

covalent bonds.

In these configurations, the other group of interactions happens between Cp or FU and SeNP (Se-A; A = O, H, N, F and C). The higher the ρ(r) and $\nabla^2\rho(r)$ values of Se-A interactions, the more stable the configuration. According to Table 3, the Se-A interactions with $-G_b/V_b > 1$, $\nabla^2\rho > 0$, $H_b > 0$, are related to weak interactions. In a more stable configuration, the number of these interactions is greater. SeCPNP/FU2 contains more than 20 Se-A with $\rho_{av} = 0.0128$ and $\nabla^2\rho_{av} = 0.040645$.

The other group of noncovalent bonds between FU and CP is hydrogen bonding. The interaction of H31 ⋯ O67 with, $E_{HB} = -18.8$ kJ mol^{-1}, $\nabla^2\rho > 0$, $H_b < 0$, $0.5 < -G_b/V_b < 1$ and the interaction of H54 ⋯ O67 with $E_{HB} = -16.2$ kJ mol^{-1}, $\nabla^2\rho > 0$, $H_b < 0$, $0.5 < -G_b/V_b < 1$ are related to the intermediate hydrogen bond. Also, the other 2 hydrogen bonds with $H_b > 0$, $\nabla^2\rho > 0$ and $-G_b/V_b > 1$ are related to the weak hydrogen bonding. Like SeCPNP FU2, the Se-A interactions in SeCPNP/FU3 with $\nabla^2\rho > 0$, $-G_b/V_b >$, $H_b > 0$ are related to weak interactions. SeCPNP/FU3 consists of 24 Se-A interactions with $\rho_{av} = 0.012577$ and $\nabla^2\rho_{av} = 0.03956$ n bonding. All 4 hydrogen bonds between FU and CP with

Table 3. Topological Parameters in a.u. for SeCPNP/FU2

Atoms	ρ(r)	$\nabla^2\rho(r)$	V_b	G_b	H_b	$-G_b/V_b$
		Se-Se interactions				
Se58-Se59	0.1122	-0.07003	-0.10012	0.04130	-0.05881	0.4125
Se57-Se58	0.11164	-0.07135	-0.09839	0.04027	-0.05811	0.4093
Se62-Se63	0.11358	-0.07471	-0.10208	0.04170	-0.06038	0.40851
Se58-Se61	0.01674	0.044954	-0.009	0.01011	0.001122	1.12473
Se60-Se63	0.01810	0.046721	-0.0097	0.010688	0.000993	1.102424
Se63-Se64	0.110076	-0.06819	-0.09577	0.03936	-0.05641	0.410998
Se58-Se63	0.012742	0.036734	-0.00693	0.008056	0.001127	1.16265
Se59-Se60	0.09917	-0.05022	-0.07831	0.032879	-0.04543	0.419841
Se60-Se61	0.114989	-0.07608	-0.10471	0.042847	-0.06187	0.409181
Se61-Se62	0.098839	-0.04757	-0.07824	0.033172	-0.04506	0.42399
Se57-Se64	0.104949	-0.0638	-0.08679	0.035418	-0.05137	0.40813
		Se-A interactions				
O22-Se58	0.015362	0.054337	-0.00986	0.011723	0.001861	1.188704
O19-Se58	0.014344	0.050211	-0.00985	0.011199	0.001354	1.137532
C9-Se59	0.012976	0.0435	-0.00765	0.009263	0.001613	1.21085
N11-Se59	0.013862	0.038048	-0.00832	0.008915	0.000597	1.071772
C12-Se58	0.010055	0.032896	-0.00544	0.006832	0.001392	1.255882
O24-Se63	0.014314	0.050291	-0.00975	0.011163	0.00141	1.144571
H29-Se57	0.015546	0.040462	-0.00921	0.009661	0.000455	1.049424
N53-Se62	0.014145	0.039605	-0.00866	0.009282	0.000619	1.071453
C48-Se62	0.015209	0.053214	-0.00975	0.011524	0.001779	1.182555
C55-Se63	0.00961	0.031158	-0.00511	0.00645	0.001339	1.261984
H52-Se64	0.00931	0.028077	-0.00451	0.005764	0.001255	1.278332
O20-Se57	0.013963	0.045128	-0.00978	0.010532	0.00075	1.076671
H42-Se59	0.010634	0.032747	-0.00576	0.006971	0.001216	1.211295
H38-Se59	0.008376	0.026637	-0.0042	0.005431	0.001229	1.29248
H45-Se62	0.012369	0.038552	-0.00697	0.008306	0.001332	1.190995
C3-Se63	0.01377	0.049774	-0.00873	0.010589	0.001855	1.212388
H47-Se64	0.012577	0.034226	-0.00701	0.007784	0.000772	1.110097
O56-Se64	0.015386	0.048927	-0.01084	0.011535	0.000697	1.064311
Se61-C72	0.011283	0.030983	-0.00536	0.006554	0.001192	1.222305
Se60-O66	0.012556	0.03875	-0.00829	0.008986	0.000701	1.084611
Se62-N68	0.014596	0.046023	-0.00872	0.010113	0.001393	1.159748
		Intermolecular hydrogen bonds				
N8-H29	0.010224	0.030761	-0.00511	0.0064	0.001291	1.252691
H31-O67	0.018246	0.054375	-0.01433	0.013963	-0.00037	0.974253
H54-O67	0.015222	0.047945	-0.01237	0.012176	-0.00019	0.984715
O21-H74	0.028538	0.095863	-0.02243	0.023198	0.000768	1.03424

Table 4. Topological Parameters in a.u. for SeCPNP/FU3

Atoms	ρ(r)	$\nabla^2\rho(r)$	V_b	G_b	H_b	$-G_b/V_b$
		Se-Se interactions				
Se62-Se63	0.112917	-0.072103	-0.101206	0.04159	-0.059616	0.41094402
Se58-Se59	0.11202	-0.06867	-0.099987	0.04141	-0.058577	0.41415384
Se57-Se58	0.111897	-0.071569	-0.098877	0.040493	-0.058384	0.40952901
Se60-Se63	0.016257	0.043136	-0.008571	0.009677	0.001106	1.12903979
Se58-Se61	0.017507	0.045747	-0.009336	0.010386	0.00105	1.11246787
Se58-Se63	0.013682	0.038703	-0.007435	0.008555	0.00112	1.15063887
Se59-Se60	0.098615	-0.047712	-0.077736	0.032904	-0.044832	0.42327879
Se60-Se61	0.113321	-0.07536	-0.101368	0.041264	-0.060104	0.40707127
Se61-Se62	0.10183	-0.052783	-0.082744	0.034774	-0.04797	0.42026008
Se63-Se64	0.112055	-0.073229	-0.098806	0.040249	-0.058557	0.4073538
Se57-Se64	0.103429	-0.061434	-0.08431	0.034476	-0.049834	0.40891946
		Se-A interactions				
O21-Se63	0.016169	0.056932	-0.010495	0.012364	0.001869	1.1780848
O22-Se58	0.016037	0.056469	-0.010381	0.012249	0.001868	1.1799441
O19-Se58	0.014987	0.053474	-0.010217	0.011793	0.001576	1.1542527
O24-Se63	0.015184	0.055042	-0.010167	0.011964	0.001797	1.1767483
N11-Se59	0.013828	0.037667	-0.00829	0.008853	0.000563	1.0679131
H41-Se57	0.010368	0.031031	-0.005218	0.006488	0.00127	1.2433882
N53-Se62	0.015384	0.042461	-0.009402	0.010009	0.000607	1.0645607
C48-Se62	0.014135	0.047907	-0.008638	0.010308	0.00167	1.1933317
H52-Se64	0.010073	0.029993	-0.005009	0.006254	0.001245	1.2485526
H29-Se57	0.014749	0.038512	-0.008589	0.009109	0.00052	1.0605425
O20-Se57	0.013294	0.043413	-0.009301	0.010077	0.000776	1.0834318
O20-Se58	0.010506	0.034398	-0.005827	0.007213	0.001386	1.2378582
H42-Se59	0.010784	0.033114	-0.005849	0.007064	0.001215	1.2077278
C9-Se59	0.012962	0.043274	-0.007614	0.009216	0.001602	1.2104018
H38-Se59	0.008149	0.025835	-0.00401	0.005234	0.001224	1.3052369
H45-Se61	0.009927	0.031838	-0.005461	0.00671	0.001249	1.2287126
H31-Se62	0.009424	0.030054	-0.004889	0.006201	0.001312	1.2683575
H45-Se62	0.01065	0.033203	-0.005817	0.007059	0.001242	1.2135121
O56-Se63	0.010052	0.032511	-0.005596	0.006862	0.001266	1.2262330
H47-Se64	0.013561	0.0359	-0.007705	0.00834	0.000635	1.0824140
O56-Se64	0.013209	0.04313	-0.009224	0.010003	0.000779	1.0844536
Se61-N68	0.010243	0.028545	-0.00572	0.006428	0.000708	1.1237762
Se61-N69	0.010362	0.030899	-0.005967	0.006846	0.000879	1.1473102
Se62-C72	0.017823	0.053972	-0.010885	0.012189	0.001304	1.1197978
		Intermolecular hydrogen bonds				
H31-F65	0.004885	0.023699	-0.003265	0.004595	0.00133	1.4073506
O49-F65	0.004799	0.025832	-0.0041	0.005279	0.001179	1.2875609
H54-F65	0.013717	0.051659	-0.012728	0.012821	0.000093	1.0073067
O49-H76	0.014297	0.05164	-0.011113	0.01201	0.00089	1.08080620

$H_b > 0$, $\nabla^2\rho > 0$ and $-G_b/V_b > 1$ are related to the weak hydrogen bonding.

CONCLUSIONS

In this study, 6 configurations (SeCPNP/FU1-6) of selenium-cyclic peptide nanocarrier with the anticancer drug of 5-fluorouracil (FU) were examined in the aqueous solution and gas phase at the M06-2X level. Cyclooctaglycine was used for cyclic peptide and Se8 octahedral selenium was employed for selenium nanoparticles modeling. Binding energy values indicate that the functionalization of SeCPNP with FU in (SeCPNP/FU1-6) is appropriate and the simultaneous drug interaction with CP and SeNP resulted in greater stability. The results obtained from solvation energies show that the solubility of SeNP and FU enhances in the vicinity of CP. The values of solvation and binding energies indicate that SeCPNP/FU2 is the most stable configuration. Binding energies, in addition to the energetic stability, indicate the amount of drug loading by the cyclic peptide anticancer nanocarrier. Therefore, due to the large amounts of binding energies, it is predicted that the amount of drug loading by this carrier is acceptable.

The energy gap of FU drug is higher than those of SeCPNP/FU1-6, showing the reactivity of drug in the vicinity of SeCPNP increases. In addition, in accordance with AIM studies, FU can be activated in SeCPNP via Se-A which (Se-A; A = O, H, N, F and C) interactions and hydrogen bonding. Se-A interactions with $\nabla^2\rho > 0$, $H_b > 0$ $-G_b/V_b > 1$ are related to weak interactions. AIM results showed that the most stable configuration has the strongest hydrogen bonds and Se-A interactions. Increasing the solubility and decreasing the toxicity of the FU drug, most of which is related to the formation of hydrogen bonds, makes this drug a good candidate for the cyclic peptide anticancer nanocarrier.

Electronic Supplementary Information

Supplementary data associated with this article can be found, in the online version, at https://doi.org/

ACKNOWLEDGEMENTS

We thank the Research Center for Animal Development Applied Biology for allocation of computer time. This research did not receive any specific grant from funding agencies in the public, commercial or not-for-profit sectors.

REFERENCES

[1] S. Fernandez-Lopez, H.-S. Kim, E.C. Choi, M. Delgado, J.R. Granja, A. Khasanov, K. Kraehenbuehl, G. Long, D.A. Weinberger, K.M. Wilcoxen, Nature 412 (2001) 452.

[2] S.C. Larnaudie, J.C. Brendel, I. Romero-Canelón, C. Sanchez-Cano, S. Catrouillet, J. Sanchis, J.P. Coverdale, J.-I. Song, A. Habtemariam, P.J. Sadler, Biomacromolecules 19 (2018) 239.

[3] A.J. Ellison, I.C. Tanrikulu, J.M. Dones, R.T. Raines, Biomacromolecules 21 (2020) 1539.

[4] A. Ortiz-Acevedo, H. Xie, V. Zorbas, W.M. Sampson, A.B. Dalton, R.H. Baughman, R.K. Draper, I.H. Musselman, G.R. Dieckmann, J. Am. Chem. Soc. 127 (2005) 9512.

[5] M. Shahabi, H. Raissi, J. Mol. Liq. 268 (2018) 326.

[6] B. Claro, M. Bastos, R. Garcia-Fandino, Peptide Applications in Biomedicine, Biotechnology and Bioengineering, Elsevier, 2018.

[7] A. Zorzi, K. Deyle, C. Heinis, Curr. Opin. Chem. Biol. 38 (2017) 24.

[8] S.E. Park, M.I. Sajid, K. Parang, R.K.M.P. Tiwari, Mol. Pharm. 16 (2019) 3727.

[9] D. Mandal, A. Nasrolahi Shirazi, K. Parang, Angew. Chem. Int. Ed. 50 (2011) 9633.

[10] X. Jing, K.J.M.R.R. Jin, Med. Res. Rev. 40 (2020) 753.

[11] P.G. Dougherty, A. Sahni, D. Pei, Chem. Rev. 119 (2019) 10241.

[12] D.B. Longley, D.P. Harkin, P.G. Johnston, Nat. Rev. Cancer 3 (2003) 330.

[13] M. Rahbar, A. Morsali, M.R. Bozorgmehr, S.A. Beyrmabadi, J. Mol. Liq. 302 (2020) 112495.

[14] M.S. Aapro, C. Martin, S. Hatty, Antcancer Drugs 9 (1998) 191.

[15] M. Najafi, A. Morsali, M.R. Bozorgmehr, Struct. Chem. (2018) 1.

[16] K. Renu, V. Abilash, T.P. PB, S. Arunachalam, Eur. J. Pharmacol. 818 (2018) 241.

835.

[17] J.D. Sara, J. Kaur, R. Khodadadi, M. Rehman, R. Lobo, S. Chakrabarti, J. Herrmann, A. Lerman, A. Grothey, Ther. Adv. Med. Oncol. 10 (2018) 1758835918780140.

[18] L. Metterle, C. Nelson, N. Patel, J. Am. Acad. Dermatol. 74 (2016) 552.

[19] J.J. Lee, J.H. Beumer, E. Chu, Cancer Chemother. Pharmacol. 78 (2016) 447.

[20] X.-S. Xian, H. Park, M.-G. Choi, J.M. Park, Anticancer Res. 33 (2013) 2541.

[21] D.C. Luther, R. Huang, T. Jeon, X. Zhang, Y.-W. Lee, H. Nagaraj, V. Rotello, Adv. Drug Deliv. Rev. 156 (2020) 188.

[22] F. Naghavi, A. Morsali, M.R. Bozorgmehr, J. Mol. Liq. 282 (2019) 392.

[23] Z. Shabani, A. Morsali, M.R. Bozorgmehr, S.A. Beyramabadi, Chem. Phys. Lett. 719 (2019) 12.

[24] S. Khani, M. Montazerzohori, R. Naghiha, S. Joohari, Inorg. Chem. Res. 4 (2020) 279.

[25] R. Ye, S. Wang, J. Wang, Z. Luo, Q. Peng, X. Cai, Y. Lin, Curr. Drug Metab. 14 (2013) 910.

[26] M. Lotfi, A. Morsali, M.R. Bozorgmehr, Appl. Surf. Sci. 462 (2018) 720.

[27] M.L. Girase, P.G. Patil, P.P. Ige, P. Biomaterials, Int. J. Polymer. Mater. 69 (2020) 990.

[28] M. Nasrabadi, A. Morsali, S.A. Beyramabadi, Int. J. Biol. Macromol. 165 (2020) 1229.

[29] B.M. Cooper, J. Iegre, D.H. O'Donovan, M.Ö. Halvarsson, D.R. Spring, Chem. Soc. Rev. (2021).

[30] Y. Zhang, H.F. Chan, K.W. Leong, Adv. Drug Deliv. Rev. 65 (2013) 104.

[31] J. Yang, E. Lee, M. Ku, Y.M. Huh, J.H. Cheong, Anticancer Agents Med. Chem. 13 (2013) 212.

[32] M. Silhol, M. Tyagi, M. Giacca, B. Lebleu, E. Vivès, Eur. J. Biochem. 269 (2002) 494.

[33] G. Yang, R. Zhou, J. Trace Elem. Electrolytes Health Dis. 8 (1994) 159.

[34] D. Wang, E.W. Taylor, Y. Wang, X. Wan, J. Zhang, Int. J. Nanomedicine 7 (2012) 1711.

[35] F. Yang, Q. Tang, X. Zhong, Y. Bai, T. Chen, Y. Zhang, Y. Li, W. Zheng, Int. J. Nanomedicine 7 (2012)

[36] F. Naghavi, A. Morsali, M.R. Bozorgmehr, S.A. Beyramabadi, J. Mol. Liq. 310 (2020) 113155.

[37] M. Nasrabadi, S.A. Beyramabadi, A. Morsali, Int. J. Biol. Macromol. 147 (2020) 534.

[38] H. Lari, A. Morsali, M.M. Heravi, Z. Phys. Chem. 232 (2018) 579.

[39] M. Teymoori, A. Morsali, M.R. Bozorgmehr, S.A. Beyramabadi, Bull. Korean Chem. Soc. 38 (2017) 869.

[40] Y.B. Zheng, B. Kiraly, T.J. Huang, Nanomedicine 5 (2010) 1309.

[41] V. Linko, A. Ora, M.A. Kostiainen, Trends Biotechnol. 33 (2015) 586.

[42] Y. Zhao, N.E. Schultz, D.G. Truhlar, J. Chem. Theory Comput. 2 (2006) 364.

[43] Y. Zhao, D.G. Truhlar, J. Chem. Phys. 125 (2006) 194101.

[44] M. Frisch, G. Trucks, H. Schlegel, G. Scuseria, M. Robb, J. Cheeseman, G. Scalmani, V. Barone, B. Mennucci, G. Petersson, Gaussian 09, Revision B.01. Gaussian, Inc., Wallingford, CT, 2009.

[45] R. Cammi, J. Tomasi, J. Comput. Chem. 16 (1995) 1449.

[46] J. Tomasi, M. Persico, Chem. Rev. 94 (1994) 2027.

[47] R.G. Parr, L.V. Szentpaly, S. Liu, J. Am. Chem. Soc. 121 (1999) 1922.

[48] T.A. Keith, TK Gristmill Software, Overland Park KS, USA, 2013.

[49] R.F. Bader, Chem. Rev. 91 (1991) 893.

[50] I.L. Li, S. Ruan, Z. Li, J. Zhai, Z. Tang, Appl. Phys. Lett. 87 (2005) 071902.

[51] J. He, W. Lv, Y. Chen, K. Wen, C. Xu, W. Zhang, Y. Li, W. Qin, W. He, ACS Nano 11 (2017) 8144.

[52] R. Poteau, G. Trinquier, J. Am. Chem. Soc. 127 (2005) 13875.

[53] Y. Zhao, D.G. Truhlar, Theor. Chem. Acc. 120 (2008) 215.

[54] I. Rozas, I. Alkorta, J. Elguero, J. Am. Chem. Soc. 122 (2000) 11154.

[55] E. Espinosa, M. Souhassou, H. Lachekar, C. Lecomte, Acta Crystallogr. Sect. B: Struct. Sci. 55 (1999) 563.